

Discovery of Aryloxy Tetramethylcyclobutanes as Novel Androgen Receptor Antagonists

Chuangxing Guo,^{*,†} Angelica Linton,^{*,†} Susan Kephart,[†] Martha Ornelas,[†] Mason Pairish,[†] Javier Gonzalez,[†] Samantha Greasley,[†] Asako Nagata,[†] Benjamin J. Burke,[†] Martin Edwards,[†] Natilie Hosea,[‡] Ping Kang,[‡] Wenyue Hu,[§] Jon Engebretsen,^{||} David Briere,^{||} Manli Shi,^{||} Hovik Gukasyan,[⊥] Paul Richardson,[†] Kevin Dack,[#] Toby Underwood,[#] Patrick Johnson,[#] Andrew Morell,[#] Robert Felstead,[#] Hidetoshi Kuruma,[▽] Hiroaki Matsimoto,[▽] Amina Zoubeidi,[▽] Martin Gleave,[▽] Gerrit Los,^{||} and Andrea N. Fanjul^{||}

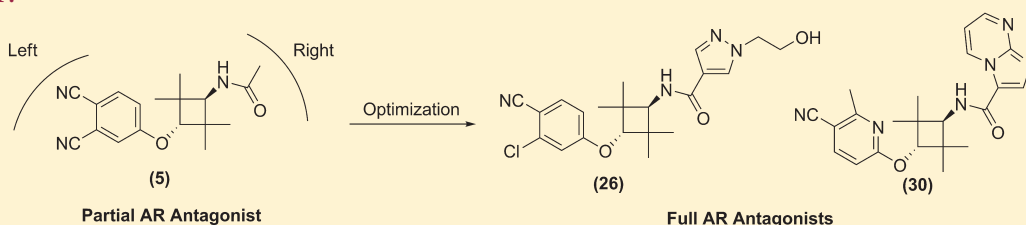
[†]Oncology Medicinal Chemistry, [‡]PDM, [§]DSRD, ^{||}Oncology Research Unit, and [⊥]Pharmaceutical Science Research Enabling Group, Pfizer Worldwide Research & Development, San Diego, California 92121, United States

[#]World-Wide Medicinal Chemistry, Pfizer Worldwide Research & Development, Sandwich, CT 13 9NJ, United Kingdom

[▽]The Vancouver Prostate Centre, University of British Columbia, 2660 Oak Street, Vancouver BC, V6H 3Z6, Canada

Supporting Information

ABSTRACT:



An aryloxy tetramethylcyclobutane was identified as a novel template for androgen receptor (AR) antagonists via cell-based high-throughput screening. Follow-up to the initial “hit” established **5** as a viable lead. Further optimization to achieve full AR antagonism led to the discovery of **26** and **30**, both of which demonstrated excellent in vivo tumor growth inhibition upon oral administration in a castration-resistant prostate cancer (CRPC) animal model.

Several androgen receptor (AR) antagonists have been used for the treatment of prostate cancer.¹ One example is bicalutamide (compound **1**, Figure 1), which was first approved as a combination therapy with surgical or medical castration for the treatment of advanced prostate cancer and subsequently launched as monotherapy for the treatment of early stage disease.² Unfortunately, a decrease in efficacy was observed after 0.5–2 years of treatment in nearly all patients undergoing either mono or combination therapy with bicalutamide. It has been suggested that the overexpression of AR is sufficient to confer resistance to hormone therapy. This phenomenon was initially called hormone refractory prostate cancer (HRPC), but it is currently more appropriately referred to as castration-resistant prostate cancer (CRPC). Elevated AR expression together with an imbalance between coactivators and corepressors are thought to be key players in the full antagonist-to-partial antagonist switch observed for existing antiandrogens such as flutamide and bicalutamide. The residual AR agonism is believed to be responsible for the observed drug resistance in CRPC patients.³ Recently, novel AR antagonists such as MDV3100 (**2**, Figure 1) and BMS-641988 (**3**) demonstrated efficacy in animal models of CRPC^{4,5} as well as clinically in CRPC patients.⁶ These encouraging results have stimulated research for a new generation of nonsteroidal pure AR antagonists directed to CRPC patients.

A CRPC cell-based high-throughput screening assay⁷ was used as the first step in our search for a second-generation novel structural class of full AR antagonists that would be efficacious against CRPC. Significant AR agonism (2.08-fold induction at 1 μ M) was observed for bicalutamide (**1**) in this assay. A corporate library of \sim 800 nuclear hormone receptor modulators (NHRM) was screened using the high-throughput assay. The aryloxy tetramethylcyclobutane alcohol **4** (Figure 2) was identified as an attractive hit, possessing potent AR antagonism with low molecular weight; however, it had residual agonism of 1.10-fold induction (FI) at 1 μ M concentration.⁸ Lead optimization of **4** to improve absorption, distribution, metabolism, and elimination (ADME) properties by reducing lipophilicity provided more ligand-efficient **5** [Figure 2, ligand efficiency based on number of heavy atoms (LE) = 0.41, ligand efficiency based on lipophilicity (LipE) = 3.48]⁹ with no apparent residual agonism at 1 μ M (0.85-fold induction). In a pharmacokinetic study (PK), compound **5** demonstrated a systemic free drug concentration covering the target ($1 \times$ free IC₅₀) for 24 h, following a single oral dose at 10 mg/kg in mice. This class of compounds tended to be metabolically stable with multiple examples in the series

Received: August 5, 2011

Published: September 21, 2011

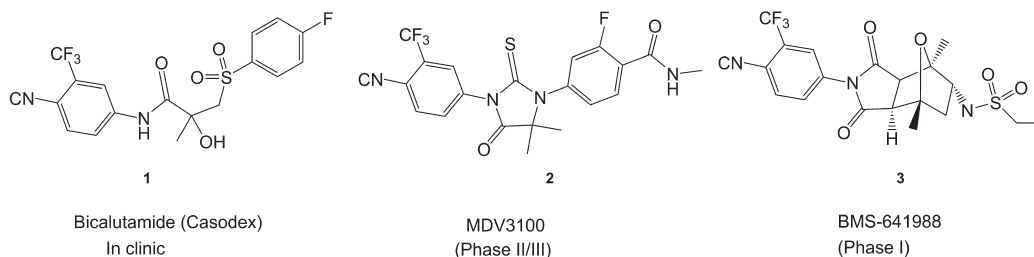


Figure 1. Known AR antagonists.

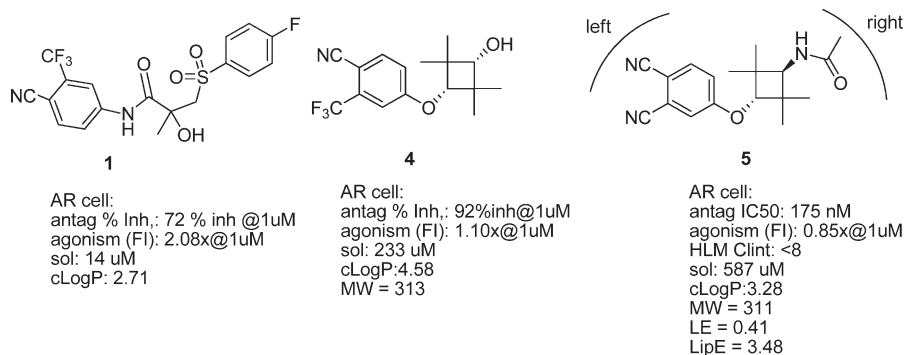


Figure 2. Initial hit and optimized lead.

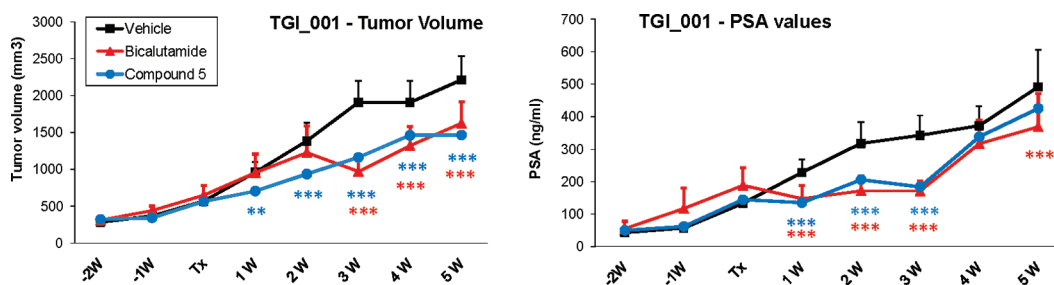


Figure 3. Effect of compound 5 on tumor growth and PSA levels in LNCaP xenograft model of CRPC. Animals were grouped and treated with vehicle ($n = 15$), 10 mg/kg bicalutamide ($n = 12$), or 10 mg/kg compound 5 ($n = 14$). Each compound was given orally once a day for 5 weeks. Compound 5 did not demonstrate statistically significant tumor volume inhibition (45%) with respect to bicalutamide (41%). PSA suppression was maximal at week 3 and comparable in both compounds (bicalutamide = 50% and 5 = 46%). There was no effect on body weight observed for these compounds during the length of study. Bars represent standard errors of the mean (SEM). Statistical significant differences between treatments = $**P < 0.01$ and $***P < 0.001$; “ n ” represents the number of animals per group. By week 5, the number of animals in each group were 8, 10, and 11 for vehicle, bicalutamide, and compound 5, respectively. Statistical analysis was done using two-way ANOVA (GraphPad Prism, Version 5.01, <http://www.graphpad.com>).

having an acceptable clearance [human liver microsomes (HLM) $Clint < 8$]¹⁰ even at high lipophilicity ($cLog P > 3$).

In a CRPC in vivo model¹¹ used to correlate PK and pharmacodynamic properties, 5 suppressed PSA, a biomarker of AR antagonism,¹² after a single oral dose of 10 mg/kg (25% reduction of PSA at 48 h). Upon daily oral administration of 10 mg/kg for 5 weeks, 5 demonstrated statistically significant tumor volume inhibition (45%). PSA suppression was maximal at week 3 (46%) with respect to vehicle control but was not sustained. After 5 weeks of treatment, PSA suppression was only 13% for compound 5 and 25% for bicalutamide (1). Although the observed in vivo efficacy from this lead was encouraging, the lack of improvement over bicalutamide in this model suggested that 5 may not have improved clinical efficacy when compared to bicalutamide in CRPC patients (Figure 3).

On the basis of the hypothesis that residual AR agonism leads to inferior efficacy in CRPC, for example, bicalutamide,³ the biological activity profile of 5 (Figure 2) was inspected more closely for any sign of residual agonism. Results from the anti-proliferation assay showed that 5 is less efficacious at a higher concentration resulting in a “V” shape dose–response curve (Figure 4). Compound 5 is highly soluble in water (sol = 587 μM), so we speculated that the nonlinear dose–response phenomenon may be due to residual AR agonism at higher concentration. Bicalutamide demonstrated a linear dose–response effect when tested in the CaP cell panel at doses up to 10 μM , but its overall weaker efficacy in inhibiting the proliferation of LNCaP cells is consistent with profile of a partial antagonist against CRPC cancer cells. Moreover, significant agonism was seen for bicalutamide (1) in the LNCaP-Luciferase assay (2.08 \times induction at 1 μM).

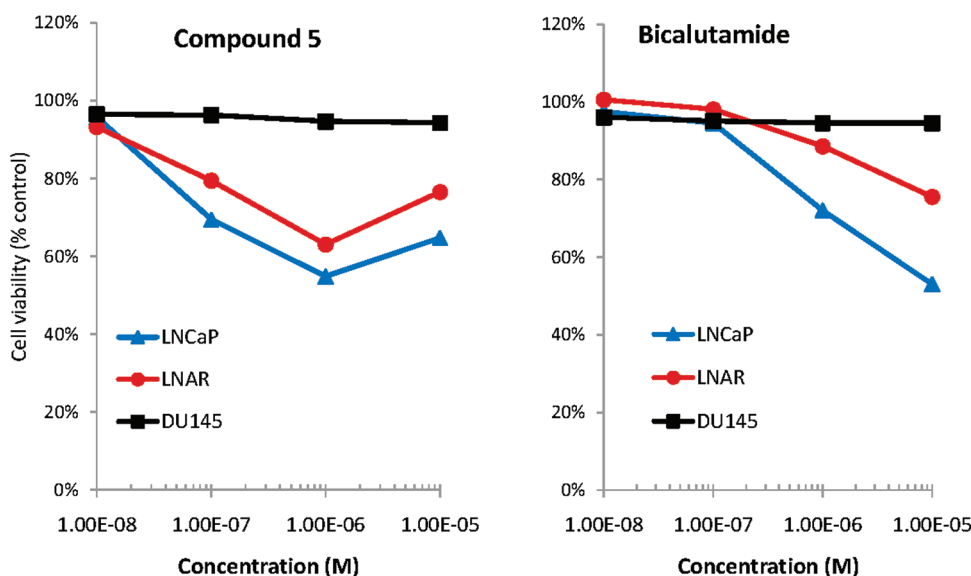


Figure 4. Antiproliferative effects of bicalutamide vs compound 5 in CaP cell panel (LNCaP, LNAR, and DU145). Cell proliferation was assessed by treating various prostate cancer (CaP) cells for 7 days in the presence of the compounds under study. The CaP panel was comprised of the following cell lines and corresponding AR status: LNCaP—mutant AR [T877A, ligand binding domain (LBD)], originated from metastatic lesion in a lymph node; LNAR—LNCaP cells engineered to express high levels of wild-type AR and the AR negative cell line, DU145. Cells were seeded in the morning in 96-well plates in RPMI containing 5% fetal bovine serum (FBS) and treated in the afternoon with the specified compounds and concentrations. On days 3 and 5, medium was changed, and compounds were replenished. On day 7, cell viability was assessed by means of a resazurin assay.

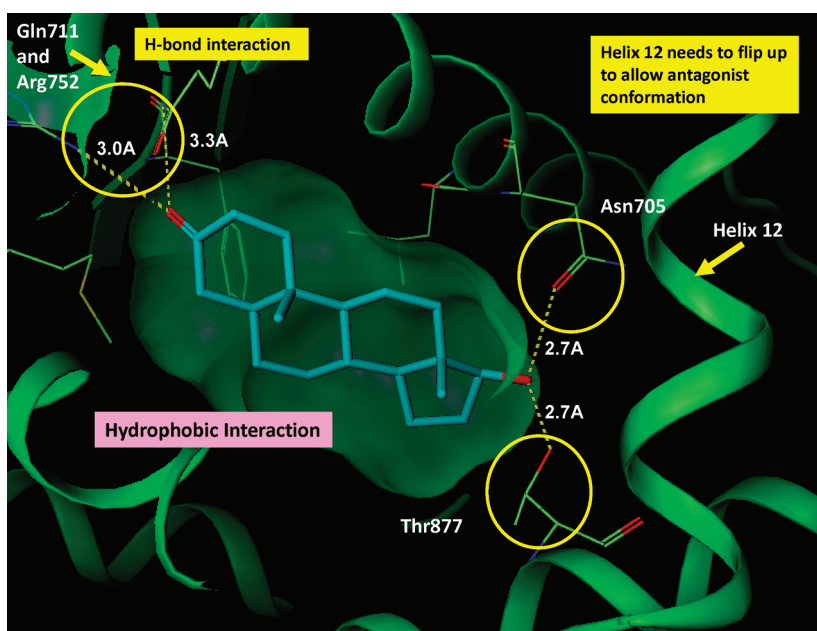


Figure 5. DHT interactions. Crystal structure (PDB: 1T7R, ref 14c) of DHT in the LBD of hAR (green backbone).

Therefore, the antiproliferation assay was incorporated into our testing cascade as an additional measure to screen out analogues possessing any residual AR agonism. The readout from the assay should help address AR specificity of our compounds (DU145 is an AR negative cell line, Figure 4).

Pereira de Jesus-Tran et al. have described the molecular determinants responsible for affinity of ligands to the AR.¹³ The AR ligand-binding domain (LBD) contains hydrophobic residues that preferably interact with lipophilic ligands such as steroidal molecules [e.g., dihydrotestosterone (DHT) or testosterone].

These residues are mobile and can adopt various conformations. Additionally, the binding site is completed by a few polar residues that firmly tether DHT/testosterone via hydrogen bond networks formed with polar atoms found at both ends of the ligand structures.¹³ It appears that interaction with Arg752 and Gln711 on one end and a hydrogen bond to Asn705 and Thr877 on the other end of the LBD constitutes the most important recognition elements for ligand affinity.¹⁴ The interaction of DHT/testosterone to Arg752 occurs via C3 ketone, whereas in bicalutamide (**1**), the interaction presumably occurs via the *p*-cyano group; hence,

this cyano moiety was kept constant in our cyclobutyl scaffold as a crucial binding element (5, Figure 2). The interaction of DHT/testosterone to Asn705 and Thr877 occurs through the 17 β hydroxyl group (Figure 5).

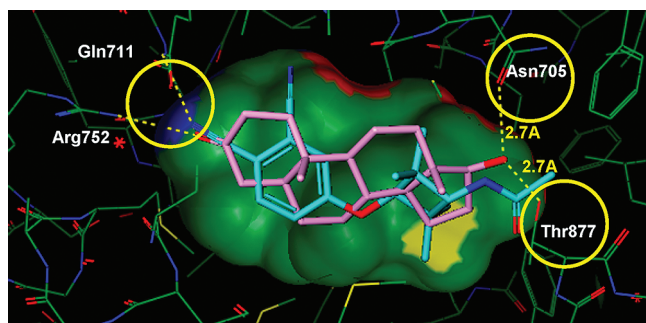
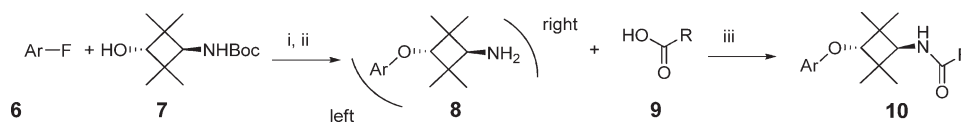


Figure 6. Compound 5 model interactions. Model of 5 (aqua) in the LBD of hAR (green backbone). DHT is shown in pink for reference.

Previous publications have described the critical role of helix 12 in conformational changes that can induce antagonism in various nuclear receptors. It has been hypothesized that pushing helix 12 into an open conformation is the mechanism leading to antagonism for estrogen receptor (ER) and other nuclear receptors.¹⁵ Because of its molecular length, 5 is unlikely to induce this conformational change. When compound 5 was modeled in AR-LBD binding site, the ligand made the crucial H-bond interactions to Arg752 through the cyano group and to Asn705 through the amide NH; however, the size of an acetate group was not large enough to “wedge” between Asn705 and Thr877 to drive the helix 12 in an open conformation (Figure 6), which may explain the residual agonism observed. On the basis of this analysis and with the knowledge that larger compounds in this series can be metabolically stable even at high Log *P*, new AR antagonists were designed to meet three key requirements: (1) form H-bond to Arg752, (2) form a H-bond to Asn705, and (3) force helix 12 into an open conformation (e.g., with a heterocyclic ring) that would wedge between Asn705 and Thr877.

Scheme 1. Synthesis of Cyclobutyl Analogues^a



^a Reagents and conditions: (i) NaH, DMF. (ii) HCl, 1,4-Dioxane. (iii) HBTU, DMF, triethylamine.

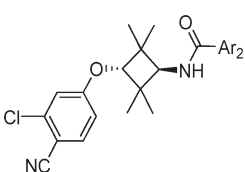
Table 1. Aryl Ether (Left-Hand Side) Optimization of Aryloxy Tetramethylcyclobutanes

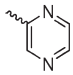
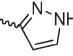
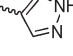
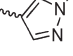
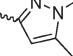
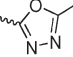
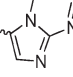
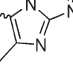
Compd	Ar ₁	Ant IC ₅₀ (nM) ^a	Agonism (FI @1 uM) ^b	HLM Clint (uL/min/mg)	ClogP	Solub (uM) ^c
5		175	0.8	<7	3.28	587
11		32	1.2	<8	4.37	9.8
12		70	0.8	<7	4.37	37
13		126	1	11	4.70	33
14		161	1	17.5	4.37	45
15		519	0.8	failed ^d	3.59	447

^a Cell-based functional assay in LNCaP cells genetically engineered to overproduce AR (ref 7). ^b Agonism reported as fold increase at 1 uM (ref 7).

^c Kinetic solubility at pH 7.4. ^d Compound 15 ionizes poorly under the MS conditions used in the HLM assay, so reliable data for this compound could not be obtained from this assay.

Table 2. Amide Portion (Right-Hand Side) Optimization of Aryloxy Tetramethylcyclobutane



Compd	Ar2	Ant IC ₅₀ (nM) ^a	Agonism (FI @1 μM) ^b	HLM Clint (uL/min/mg)	ClogP
16		82	1.1	9.8	4.76
17		75	0.7	failed ^c	4.91
18		42	1.4	<8	4.91
19		20	1.4	9	4.48
20		54	0.9	40	4.75
21		30	1.6	29	3.81
22		16	2.8	<10	5.28
23		69	0.8	19	5.21

^a Cell-based functional assay in LNCaP cells genetically engineered to overproduce AR (ref 7). ^b Agonism reported as fold increase at 1 μM (ref 7). ^c Compound 17 ionizes poorly under the MS conditions used in the HLM assay, so reliable data for this compound could not be obtained from this assay.

The preparation of the cyclobutyl analogues is outlined in Scheme 1. Synthesis began with the nucleophilic displacement of various commercially available aryl fluorides **6** with the anion of Boc-protected cyclobutyl amino alcohol **7**,¹⁶ followed by protecting group cleavage under acidic conditions to yield products **8**, which were coupled with various carboxylic acids **9** to provide the general structure **10** in good yields. The synthesis was amenable to a library format.

The availability of lipophilic space prompted us to perform an initial structure–activity relationship (SAR) investigation around the aryl ether (left-hand side) to maximize the protein–ligand van der Waals interactions to boost potency. For this experiment, the amide portion (right-hand side) was fixed as an acetate, which provides a more ligand efficient template (low MW and cLog *P*). As summarized in Table 1, 3-chloro-4-cyanophenyl in **11** (IC₅₀ = 32 nM) provided good cell-based antagonism but with residual

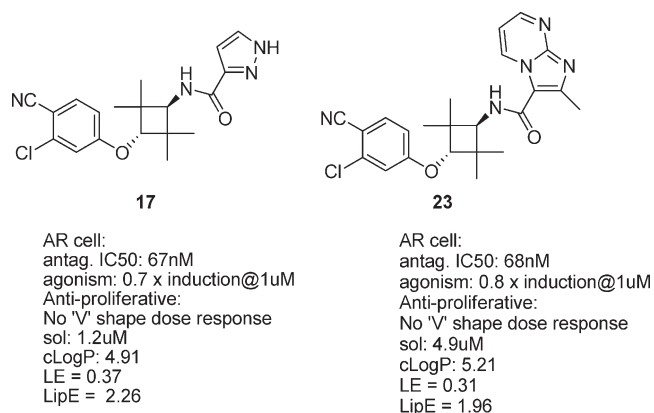


Figure 7. Physicochemical and biological properties of **17** and **23**.

agonism (1.2 fold induction at 1 μM). Although stable in HLM,¹⁰ the fragment has a high cLog *P*, which may contribute to the observed lower solubility (9.8 μM). It is worth noting that apart from the original lead compound **5**, the analogue with a pyridine group (**15**) demonstrated good overall ADME properties (lower cLog *P* and good solubility) comparable to compound **5** without any residual agonism.

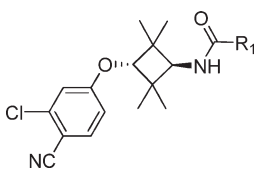
Next, the amide portion (right-hand side) group was optimized for potent AR antagonism. Several selected aryl ethers (left-hand side) from Table 1 including the ones with the highest ligand efficiency, dicyano phenyl (LipE = 3.38)⁹ in **5** and 3-chloro-4-cyanophenyl (LipE = 3.12) in **11**, were matched with various heterocyclic carboxyl amides in a library format (Table 2, only the most potent 3-chloro-4-cyanophenyl analogs are shown). Heteroaryl groups were selected based on their potentials to form additional H-bond interactions and to produce a “wedge effect” at the amide portion (right-hand side) with which to force Helix 12 into the open conformation.

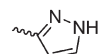
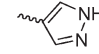
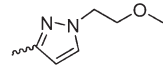
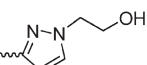
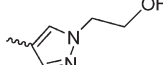
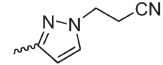
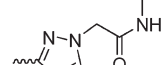
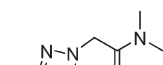
In general, the dicyano phenyl analogues (not shown) were less potent in the AR cell-based antagonist assay than the corresponding 3-chloro-4-cyanophenyl analogues. Both pyrazole **17** and 3-substituted imidazo[1,2-*a*]pyrimidin-3-yl **23** emerged as two preferred groups off the right-hand amide for potent full AR antagonism (Figure 7).⁸

Both leads **17** and **23** demonstrated moderate metabolic stability and low solubility, likely due to high lipophilicity (cLog *P* ~ 5). Therefore, subsequent analogues were designed with lower lipophilicity aiming for improved ADME characteristics. On the basis of the activity data of compound **20** (Table 2), substitution(s) off C3 and/or N4 positions of pyrazole groups were tolerated. As such, a series of analogues of **17** and **18** were designed where their pyrazole was substituted with small polar fragments (right-hand side) (Table 3). The extended design was intended not only to improve solubility but also to re-enforce the open helix 12 conformation due to additional length and solvating the terminal polar groups (e.g., amide, alcohol, or cyano groups). Among them, hydroxyethyl substitution such as **26** afforded improved solubility and good metabolic stability, while maintaining potent full AR antagonism.

Analogues of **23** (Table 2) with lower lipophilicity were designed and synthesized. Combined chemistry tactics of incorporating the pyridine aryl ether (left-hand side) (seen from **15**) and removing the methyl group from the 2-position of the imidazo[1,2-*a*]pyrimidine bicyclic ring led to **30** (Figure 8). By modestly improving LipE,⁹ both solubility and metabolic stability

Table 3. Incorporation of Polar Fragments to 17 and 18



Compd	R1	Ant IC ₅₀ (nM) ^a	Agonism (FI @ 1 μM) ^b	HLM Clint (uL/min/mg)	ClogP	Solub (uM) ^c
17		75	0.7	failed ^d	4.91	1.20
18		42	1.4	<8	4.91	8
24		136	0.9	57	4.55	39
25		136	0.8	<12	3.79	4.8 ^e
26		59	1.03	11	3.79	12 ^e
27		90	0.8	25	4.08	27
28		163	0.7	failed ^d	3.59	24.8
29		174	0.88	15	4.02	235

^a Cell-based functional assay in LNCaP cells genetically engineered to overproduce AR (ref 7). ^b Agonism reported as fold increase at 1 μM (ref 7). ^c Kinetic solubility at pH 7.4. ^d Compounds 17 and 28 ionize poorly under the MS conditions used in the HLM assay, so reliable data for this compound could not be obtained from this assay. ^e Thermodynamic solubility.

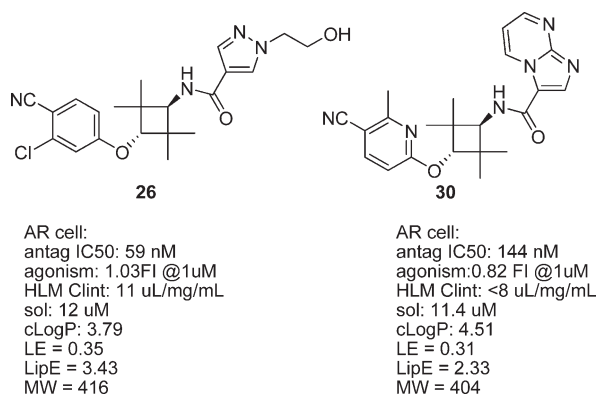


Figure 8. Optimized aryl ether (left-hand side) and amide portion (right-hand side).

were improved. In addition, the compounds have an acceptable clearance (HLM Clint <15)¹⁰ despite their high Log P.

Compounds 26 and 30 were further evaluated for their antiproliferation effects the CaP cell panel (Figure 9). The results obtained indicated that compound 30 was the more potent of the

two, with significant cell growth inhibition effects shown for LNCaP and LNCAR cells but potentially having some off-target toxicity at the highest dose tested (10 μM), as indicated by the inhibition of DU145 (AR-negative) cells when treated with 10 μM dose. Although compound 26 was less potent than compound 30, it did not appear to have any off-target effect at 10 μM, as judged by the lack of response in the AR negative cell line.

Pilot PK studies in mice suggested that both 26 and 30 (Figure 8) had the required PK profile to support oral dosing. As a result, they were chosen for further evaluation in tumor PK/pharmacodynamic (PD) and efficacy models.

In the LNCaP-derived CRPC animal tumor model,¹¹ both 26 and 30 demonstrated outstanding efficacy in inhibiting tumor growth. At the given doses, 26 [100 mg/kg once a day dosing (QD), unbound $C_{ave} = 0.22 \mu\text{M} \sim 3.7 \times \text{IC}_{50}$]¹⁷ and 30 (25 mg/kg QD, unbound $C_{ave} = 0.62 \mu\text{M} 4.5 \times \text{IC}_{50}$)¹⁷ nearly completely suppressed tumor growth (by 90 and 97%, respectively) and the PSA levels (78 and 90%, respectively) after 5 weeks (Figure 10), with no detectable body weight loss for the period of time when animals were treated. It is worth noting that at the treatment dose (25 mg/kg QD), the systemic drug exposure of compound 30 (unbound $C_{ave} = 0.62 \mu\text{M}$)¹⁷ is significantly lower

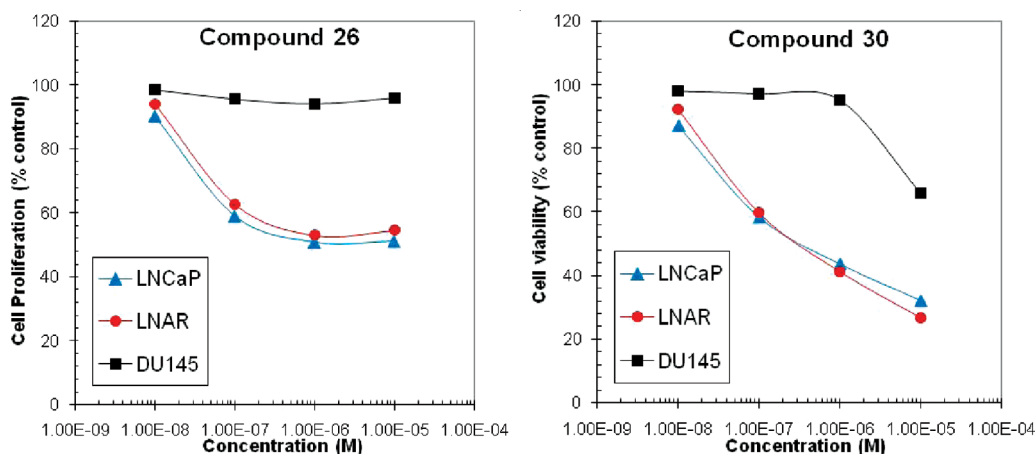


Figure 9. Antiproliferative effects of compounds 26 and 30 in CaP cell panel (LNCaP, LNA, and DU145). Cell proliferation was assessed by treating various prostate cancer (CaP) cells for 7 days in the presence of the compounds under study (see also the Figure 4 legend).

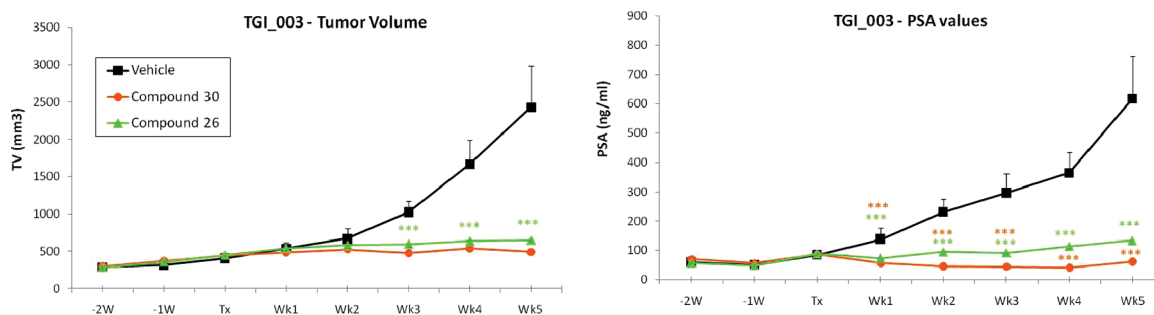


Figure 10. Effect of compounds 26 and 30 on tumor growth and PSA levels in the LNCaP xenograft mouse model of CRPC. Animals were grouped and treated with vehicle ($n = 8$), 100 mg/kg compound 26 ($n = 10$), or 25 mg/kg compound 30 ($n = 11$). Each compound was given orally once a day for 5 weeks. There was no effect on body weight observed for these compounds during the length of study. Statistical significant differences between treatments = *** $P < 0.001$. Bars represent the SEM; “ n ” represent the number of animals per group. Statistical analysis was done using two-way ANOVA (GraphPad Prism, Version 5.01, <http://www.graphpad.com>).

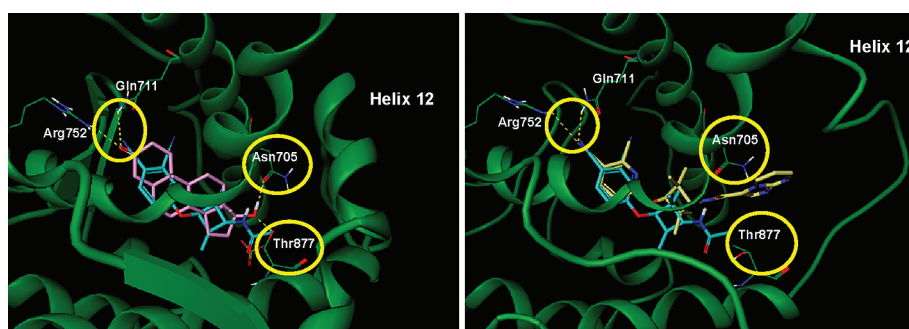


Figure 11. Compound 30 likely to induce helix 12-open conformation. Left picture: Modeled binding conformation of compound 5 (aqua), which fits AR helix 12-closed conformation vs bound conformation of DHT in crystal structure (pink, PDB: 1T7R, ref 14c). Right picture: Modeled binding conformation of compound 30 (yellow) in AR helix 12-open conformation (see the Experimental Section for more details).

than 10 μM , the concentration where there was an indication of potential off-target effects in the anti-proliferation assay.

Compound 30 is not easily accommodated in the AR LBD site model based on the cocrystal structure of AR and bicalutamide, a helix 12-closed (“closed”) conformation. Unlike the shorter analogue 5 that can fit into the “closed” conformation reasonably well (Figure 11, left), compound 30 cannot be accommodated

into the closed conformation without significant clashes with helix 12 of AR protein. To model the AR antagonists with a longer right-hand groups (e.g., 26 and 30), a helix 12-open (“open”) AR homology model was created based on the Raloxifene-bound ER crystal structure (Raloxifene is a full antagonist; PDB code: 1ERR) in which helix 12 is disrupted and adopts what we call the “open” conformation. As shown in Figure 11 (right),

compound **30** can be accommodated in the LBD site when helix 12 moves out of the way. As discussed earlier, DHT has a 17 β hydroxyl group that functions as a “latch”, which favors a helix 12-closed (agonistic) conformation by forming key hydrogen bonds to Asn705 and Thr877 simultaneously. Compound **5** lacks the “latch” interactions, but the small right-hand group (acetamide) can fit into the closed conformation. As a result, AR may adopt either the open or the closed conformation with compound **5** bound, consistent with observed its partial antagonism. However, compound **30** is not only devoid of the “latch” interactions but also contains a large right-hand group. The combined structural features strongly favor the helix 12-open conformation, presumably leading to AR full antagonism.

In summary, a series of novel nonsteroidal pure AR antagonists were developed from leads identified through cell-based high-throughput screening. The initial aryloxy tetramethylcyclobutyl leads demonstrated good AR antagonism potency and ADME profile, but only moderate efficacy in inhibiting tumor growth in a CRPC animal model, similar to results obtained with bicalutamide. Utilizing a hypothesis of full AR antagonism based on protein conformation of helix 12, a protein-structure-guided library led to the identification of pyrazole and imidazo[1,2-*a*]-pyrimidin-3-yl as preferred moieties for potent AR full antagonism. Further optimization of ligand efficiency led to the discovery of **26** and **30**, which demonstrated favorable efficacy in the CRPC model upon oral administration. The attractive in vivo efficacy and ADME profiles of these analogues warrant further evaluation for their potential use as oral agents to treat CRPC patients in the clinic.

EXPERIMENTAL SECTION

General. All starting materials and chemicals reagents were purchased from commercial suppliers and used without further purification, unless otherwise indicated. ^1H NMR spectra were recorded on a Bruker instrument operating at 400 or 600 MHz. NMR spectra are obtained as CDCl_3 , $\text{DMSO}-d_6$ solutions (reported in ppm), using CDCl_3 as the reference standard (7.25 ppm), or $\text{DMSO}-d_6$ (2.50 ppm). Other NMR solvents were used as needed. The mass spectra were obtained using LC/MS or HRMS. The purity of all final compounds was determined to be at least 95% pure by a combination of HPLC, LCMS, NMR (no extra peaks in the proton NMR spectrum), and combustion analysis (all final compounds have satisfying CHN results consistent with high purity).

General Procedure for the Preparation of Cyclobutyl Analogues. *Preparation of 30:* *N*-[*trans*-3-[(5-Cyano-6-methylpyridin-2-yl)oxy]-2,2,4,4-tetramethylcyclobutyl]imidazo[1,2-*a*]pyrimidine-3-carboxamide. **Step 1.** 6-((1*R*,3*R*)-3-Amino-2,2,4,4-tetramethylcyclobutoxy)-2-methylnicotinonitrile Hydrochloride. To a cooled stirred solution of compound **7** (4.8 g, 19.7 mmol)¹⁶ in anhydrous THF (80 mL) was added NaH (1.6 g, 39.4 mmol) in portions and at a temperature below 10 °C. After the addition, the mixture was stirred at room temperature for 30 min. Then, the reaction mixture was cooled to 10 °C, and 6-fluoro-2-methylnicotinonitrile (Ryan Scientific, PCS5881) (3.2 g, 23.6 mmol) was added in portions. After the addition, the resulting mixture was stirred at reflux for 1 h under N_2 . TLC (4:1 petroleum ether/EtOAc) showed the reaction was complete. The reaction was cooled to room temperature and quenched with cold water (10 mL). The resulting mixture was evaporated, and the residue was diluted with EtOAc (100 mL) and water (100 mL). The organic layer was separated, and the aqueous layer was re-extracted with EtOAc (100 mL \times 2). The combined organic layers were washed with brine (50 mL), dried over Na_2SO_4 , filtered, and evaporated to give the crude product, which was purified by column chromatography (20:1 to 10:1 petroleum ether/EtOAc) to

give intermediate Boc-protected intermediate: *tert*-butyl(1*R*,3*R*)-3-(5-cyano-6-methylpyridin-2-yloxy)-2,2,4,4 tetramethylcyclobutylcarbamate (4.2 g, 59%) as a white solid. ^1H NMR (CDCl_3 , 400 MHz): δ 7.70 (d, 1 H), 6.67 (d, 1 H), 4.70 (d, 1 H), 4.60 (s, 1 H), 3.62 (d, 1 H), 2.61 (s, 3 H), 1.45 (s, 9 H), 1.16 (s, 6 H), 1.10 (s, 6 H).

To a stirred solution of above intermediate *tert*-butyl(1*R*,3*R*)-3-(5-cyano-6-methylpyridin-2-yloxy)-2,2,4,4 tetramethylcyclobutylcarbamate (5.8 g, 16.1 mmol) in anhydrous dioxane (60 mL) was added 4 N HCl/dioxane (80 mL) dropwise at 5 °C. After the addition, the resulting mixture was stirred at room temperature for 3 h. The suspension was filtered, and the filter cake was washed with 10:1 petroleum ether/EtOAc (50 mL) and dried in vacuo to give the HCl salt of the title compound (4.80 g, 91%) as a white solid. ^1H NMR (D_2O , 400 MHz): δ 7.93 (d, 1 H), 6.78 (d, 1 H), 4.69 (s, 1 H), 3.29 (s, 1 H), 2.55 (s, 3 H), 1.31 (s, 6 H), 1.11 (s, 6 H). MS (APCI): 260.2 ($\text{M} + \text{H}$)⁺.

Step 2. Coupling Reaction: *N*-((1*R*,3*R*)-3-(5-Cyano-6-methylpyridin-2-yloxy)-2,2,4,4-tetramethylcyclobutyl)imidazo[1,2-*a*]pyrimidine-3-carboxamide (**30**). 6-((1*R*,3*R*)-3-Amino-2,2,4,4-tetramethylcyclobutoxy)-2-methylnicotinonitrile hydrochloride (70.0 mg, 0.237 mmol, 1.00 equiv), imidazo[1,2-*a*]pyrimidine-3-carboxylic acid (Ryan Scientific, CA10088) (44.9 mg, 0.275 mmol, 1.16 equiv), and 2-(1*H*-benzotriazole-1-yl)-1,1,3,3-tetramethyluronium hexafluorophosphate (HBTU, VWR, TCB1657) (113.9 mg, 0.29 mmol, 1.2 equiv) were dissolved in 1.0 mL of DMF (0.237 M). Triethylamine (0.10 mL 0.72 mmol, 3.0 equiv) was added, and the reaction was stirred at room temperature for 2.5 h. LCMS after 2 h at room temperature shows clean conversion to amide coupling product [MS (APCI): 405 ($\text{M} + \text{H}$)⁺, $R_f = 0.16$ in 100% EtOAc, UV⁺]. The reaction was partitioned between 10 mL of deionized water and 20 mL of ethyl acetate. The organic layer was washed with 5 mL of saturated aqueous NaCl, dried over magnesium sulfate, filtered, and concentrated to 131.9 mg of a yellow wax, which was dissolved in ethyl acetate, adsorbed on silica, and purified on a 12 g silica column, eluting with 100% ethyl acetate. The corresponding fractions were combined and concentrated in vacuo to afford the product as a white solid, 62.8 mg (66%). ^1H NMR (400 MHz, $\text{DMSO}-d_6$): δ 1.15 (s, 6 H), 1.25 (s, 6 H), 2.58 (s, 3 H), 4.12 (d, $J = 9.60$ Hz, 1 H), 4.79 (s, 1 H), 6.88 (d, $J = 8.59$ Hz, 1 H), 7.26 (dd, $J = 6.95, 4.17$ Hz, 1 H), 7.95 (d, $J = 9.60$ Hz, 1 H), 8.07 (d, $J = 8.59$ Hz, 1 H), 8.67–8.73 (m, 2 H), 9.70 (dd, $J = 6.95, 1.89$ Hz, 1 H). HRMS: [$\text{M} + \text{H}$]⁺ calcd, 405.203351; found, 405.202098; error –3.09 ppm. Anal. calcd for $\text{C}_{22}\text{H}_{24}\text{N}_6\text{O}_2 \cdot \text{cdt} \cdot 0.5 \text{H}_2\text{O}$: C, 63.91; H, 6.09; N, 20.32. Found: C, 63.85; H, 5.92; N, 20.28.

Characterization of Final Analogues. *Preparation of 5:* *N*-[*trans*-3-(3,4-Dicyanophenoxy)-2,2,4,4-tetramethylcyclobutyl]acetamide. **Step 1.** The intermediate amine was prepared by the method of compound **30**, using 4-fluorophthalonitrile (Aldrich, 47410) in step 1.

Step 2. The resultant 4-((1*R*,3*R*)-3-amino-2,2,4,4-tetramethylcyclobutoxy) phthalonitrile from step 1 above (0.5 g, 1.0 mmol) was dissolved in CH_2Cl_2 (13 mL) and triethylamine (0.290 g, 0.399 mL, 2.87 mmol, 2.2 equiv) was added followed by acetyl chloride (0.133 g, 0.120 mL, 1.3 equiv). This mixture was stirred at room temperature for 30 min. The CH_2Cl_2 was evaporated, and the residue was partitioned between EtOAc (50 mL) and 1 M sodium hydroxide (10 mL). The organic layer was separated, washed with 1 M HCl (20 mL), and then dried over Na_2SO_4 and evaporated under reduced pressure to get a yellow oil, which was adsorbed on silica, and purified on a 12 g silica column, eluting with 60% EtOAc/heptanes. The corresponding fractions were combined and concentrated in vacuo to afford the product **5** (0.44 g, quantitative) as a white solid. ^1H NMR (400 MHz, CDCl_3): δ 1.16 (s, 6 H), 1.22 (s, 6 H), 2.06 (s, 3 H), 3.99–4.04 (m, 2 H), 5.52 (d, $J = 7.83$ Hz, 1 H), 7.12 (dd, $J = 8.84, 2.53$ Hz, 1 H), 7.19 (d, $J = 2.53$ Hz, 1 H), 7.70 (d, $J = 8.59$ Hz, 1 H). MS (APCI): 312.2 ($\text{M} + \text{H}$)⁺. Anal. calcd for $\text{C}_{18}\text{H}_{21}\text{N}_3\text{O}_2$: C, 69.43; H, 6.80; N, 13.49; N, 20.32. Found: C, 69.47; H, 6.86; N, 13.37.

Preparation of 11: *N*-[*trans*-3-(3-Chloro-4-cyanophenoxy)-2,2,4,4-tetramethylcyclobutyl]acetamide. Compound **11** was prepared by

the method of compound **5**, using 2-chloro-4-fluoro-benzonitrile (Aldrich, 344265) in step 1. $^1\text{H NMR}$ (400 MHz, CDCl_3): δ 7.56 (d, 1H), 6.94 (s, 1H), 6.79 (d, 1H), 5.47 (bd, 1H), 3.97 (d, 2H), 2.04 (s, 3H), 1.19 (s, 6H), 1.16 (s, 6H). MS (APCI): 321 (M + H)⁺. Anal. calcd for $\text{C}_{17}\text{H}_{21}\text{ClN}_2\text{O}_2 \cdot 0.1\text{H}_2\text{O}$: C, 63.29; H, 6.62; N, 8.68. Found: C, 63.10; H, 6.42; N, 8.45.

Preparation of 12: *N*-[*trans*-3-(4-Cyano-3-methylphenoxy)-2,2,4,4-tetramethylcyclobutyl]acetamide. Compound **12** was prepared by the method of compound **5**, using 4-fluoro-2-methylbenzonitrile (Aldrich, 594660) in step 1. $^1\text{H NMR}$ (400 MHz, CDCl_3): δ 0.97–1.38 (m, 12H), 2.02–2.10 (m, 3H), 2.51 (s, 3H), 3.78–4.12 (m, 2H), 5.51 (s, 1H), 6.58–6.82 (m, 2H), 7.50 (d, J = 8.59 Hz, 1H). MS (APCI): 301.2 (M + H)⁺. Anal. calcd for $\text{C}_{18}\text{H}_{24}\text{N}_2\text{O}_2 \cdot 1.0\text{H}_2\text{O}$: C, 67.90; H, 8.23; N, 8.80. Found: C, 67.72; H, 8.04; N, 8.67.

Preparation of 13: *N*-[*trans*-3-(4-Cyano-3-(trifluoromethyl)phenoxy)-2,2,4,4-tetramethylcyclobutyl]acetamide. Compound **13** was prepared by the method of compound **5**, using 4-fluoro-2-trifluoromethylbenzonitrile (Alfa Aesar, B20617) in step 1. $^1\text{H NMR}$ (400 MHz, CDCl_3): δ 7.74 (d, J = 8.34 Hz, 1H), 7.29 (d, J = 2.53 Hz, 1H), 7.10 (dd, J = 8.59, 2.53 Hz, 1H), 4.92 (s, 1H), 3.84 (s, 1H), 1.57 (s, 4H), 1.32 (s, 6H), 1.25 (s, 6H). MS (APCI): 355.2 (M + H)⁺. HRMS: [M + H]⁺ calcd, 354.155510; found, 354.152381. Anal. calcd for $\text{C}_{18}\text{H}_{21}\text{F}_3\text{N}_2\text{O}_2 \cdot 0.25\text{H}_2\text{O}$: C, 60.24; H, 6.04; N, 7.81. Found: C, 60.15; H, 5.89; N, 7.75.

Preparation of 14: *N*-[*trans*-3-(2-Chloro-4-cyanophenoxy)-2,2,4,4-tetramethylcyclobutyl]acetamide. Compound **14** was prepared by the method of compound **5**, using 3-chloro-4-fluorobenzonitrile (Aldrich, 376582) in step 1. $^1\text{H NMR}$ (400 MHz, CDCl_3): δ 7.67 (d, J = 2.02 Hz, 1H), 7.49 (dd, J = 8.59, 2.02 Hz, 1H), 6.73 (d, J = 8.59 Hz, 1H), 5.50 (d, J = 6.57 Hz, 1H), 3.99–4.08 (m, 2H), 2.06 (s, 3H), 1.21 (s, 6H), 1.21 (s, 6H). MS (APCI): 321 (M + H)⁺. Anal. calcd for $\text{C}_{17}\text{H}_{21}\text{ClN}_2\text{O}_2 \cdot 1.0\text{H}_2\text{O} \cdot 0.3\text{AcOH}$: C, 59.24; H, 6.84; N, 7.85. Found: C, 59.01; H, 6.59; N, 8.05.

Preparation of 15: *N*-[*trans*-3-(5-Cyano-6-methylpyridin-2-yl)oxy]-2,2,4,4-tetramethylcyclobutyl]acetamide. Compound **15** was prepared by the method of compound **5**, using 6-fluoro-2-methylnicotinonitrile (Ryan Scientific, PCS881) in step 1. $^1\text{H NMR}$ (400 MHz, $\text{DMSO}-d_6$): δ 7.97 (d, J = 8.59 Hz, 1H), 7.49 (d, J = 9.09 Hz, 1H), 6.76 (d, J = 8.59 Hz, 1H), 4.51 (s, 1H), 3.73 (d, J = 9.35 Hz, 1H), 2.47 (s, 3H), 1.82 (s, 3H), 1.04 (s, 6H), 0.94 (s, 6H). MS (APCI): 302 (M + H)⁺. HRMS: [M + H]⁺ calcd, 302.186303; found, 302.186859. Anal. calcd for $\text{C}_{17}\text{H}_{23}\text{N}_3\text{O}_2$: C, 67.75; H, 7.69; N, 13.94. Found: C, 67.68; H, 7.57; N, 13.93.

Preparation of 16: *N*-[*trans*-3-(3-Chloro-4-cyanophenoxy)-2,2,4,4-tetramethylcyclobutyl]pyrazine-2-carboxamide. Compound **16** was prepared by the method of compound **30**, using 2-chloro-4-fluoro-benzonitrile in step 1 and pyrazine-2-carboxylic acid (Fluka, 82611) in step 2. $^1\text{H NMR}$ (400 MHz, $\text{DMSO}-d_6$): δ 1.15 (s, 6H), 1.23 (s, 6H), 4.02 (d, J = 9.09 Hz, 1H), 4.45 (s, 1H), 7.03 (dd, J = 8.84, 2.27 Hz, 1H), 7.24 (d, J = 2.27 Hz, 1H), 7.90 (d, J = 8.59 Hz, 1H), 8.26 (d, J = 9.09 Hz, 1H), 8.79 (s, 1H), 8.92 (d, J = 2.53 Hz, 1H), 9.21 (s, 1H). HRMS: [M + H]⁺ calcd, 385.14258; found, 385.1429; error, 0.83 ppm. Anal. calcd for $\text{C}_{20}\text{H}_{21}\text{ClN}_4\text{O}_2 \cdot 0.25\text{H}_2\text{O}$: C, 61.69; H, 5.57; N, 14.39. Found: C, 61.75; H, 5.45; N, 14.33.

Preparation of 17: *N*-[*trans*-3-(3-Chloro-4-cyanophenoxy)-2,2,4,4-tetramethylcyclobutyl]-1H-pyrazole-3-carboxamide. Compound **17** was prepared by the method of compound **30**, using 2-chloro-4-fluoro-benzonitrile (Aldrich, 344265) in step 1 and 1H-pyrazole-3-carboxylic acid (Aldrich, 707384) in step 2. $^1\text{H NMR}$ (400 MHz, CDCl_3): δ 1.22 (s, 6H), 1.29 (s, 6H), 4.07 (s, 1H), 4.16 (d, J = 8.59 Hz, 1H), 6.82 (dd, J = 8.72, 2.40 Hz, 1H), 6.89 (d, J = 2.53 Hz, 1H), 6.98 (d, J = 2.53 Hz, 1H), 7.10 (br. s., 1H), 7.57 (d, J = 8.59 Hz, 1H), 7.63 (d, J = 2.27 Hz, 1H), 10.29 (br. s., 1H). MS (APCI): 373.2 (M + H)⁺. Anal. calcd for $\text{C}_{19}\text{H}_{21}\text{ClN}_4\text{O}_2$: C, 61.21; H, 5.68; N, 15.03. Found: C, 61.09; H, 5.72; N, 14.90.

Preparation of 18: *N*-[*trans*-3-(3-Chloro-4-cyanophenoxy)-2,2,4,4-tetramethylcyclobutyl]-1H-pyrazole-4-carboxamide. Compound **18**

was prepared by the method of compound **30**, using 2-chloro-4-fluoro-benzonitrile in step 1 and 1-(tetrahydro-pyran-2-yl)-1H-pyrazole-4-carboxylic acid (Anichem, K11582) in step 2. After silica gel chromatography, the THP group was then removed by treatment with excess 4.0 M HCl/dioxane solution at room temperature for 18 h. The resulting monohydrochloride salt was collected by suction filtration. $^1\text{H NMR}$ (400 MHz, $\text{DMSO}-d_6$): δ 1.10 (s, 6H), 1.21 (s, 6H), 4.05 (d, J = 9.35 Hz, 1H), 4.30 (s, 1H), 7.00 (dd, J = 8.72, 2.40 Hz, 1H), 7.21 (d, J = 2.53 Hz, 1H), 7.34 (d, J = 9.35 Hz, 1H), 7.90 (d, J = 8.84 Hz, 1H), 8.14 (s, 2H). HRMS: [M + H]⁺ calcd, 373.14258; found, 373.14173; error, -2.28 ppm. Anal. calcd for $\text{C}_{19}\text{H}_{21}\text{ClN}_4\text{O}_2 \cdot 1.75\text{H}_2\text{O} \cdot 1.0\text{HCl}$: C, 51.77; H, 5.83; N, 12.71. Found: C, 51.68; H, 6.03; N, 12.42.

Preparation of 19: *N*-[*trans*-3-(3-Chloro-4-cyanophenoxy)-2,2,4,4-tetramethylcyclobutyl]-1-methyl-1H-pyrazole-4-carboxamide. Compound **19** was prepared by the method of compound **30**, using 2-chloro-4-fluoro-benzonitrile in step 1 and 1-methyl-1H-pyrazole-4-carboxylic acid (Anichem, K11201) in step 2. $^1\text{H NMR}$ (400 MHz, $\text{DMSO}-d_6$): δ 1.10 (s, 6H), 1.20 (s, 6H), 3.86 (s, 3H), 4.04 (d, J = 9.35 Hz, 1H), 4.29 (s, 1H), 7.00 (dd, J = 8.84, 2.53 Hz, 1H), 7.21 (d, J = 2.27 Hz, 1H), 7.31 (d, J = 9.35 Hz, 1H), 7.90 (t, J = 4.29 Hz, 2H), 8.25 (s, 1H). HRMS: [M + H]⁺ calcd, 387.15823; found, 387.157169; error, -2.74 ppm. Anal. calcd for $\text{C}_{20}\text{H}_{23}\text{ClN}_4\text{O}_2 \cdot 0.75\text{H}_2\text{O} \cdot 0.25\text{AcOH}$: C, 59.27; H, 6.19; N, 13.49. Found: C, 59.31; H, 6.26; N, 13.65.

Preparation of 20: *N*-[*trans*-3-(3-Chloro-4-cyanophenoxy)-2,2,4,4-tetramethylcyclobutyl]-1,5-dimethyl-1H-pyrazole-3-carboxamide. Compound **20** was prepared by the method of compound **30**, using 2-chloro-4-fluoro-benzonitrile (Aldrich, 344265) in step 1 and 1,5-dimethyl-1H-pyrazole-3-carboxylic acid (Aldrich, 722359) in step 2. $^1\text{H NMR}$ (400 MHz, CDCl_3): δ 1.21 (s, 6H), 1.28 (s, 6H), 2.30 (s, 3H), 3.81 (s, 3H), 4.06 (s, 1H), 4.12 (d, J = 8.59 Hz, 1H), 6.55 (s, 1H), 6.81 (d, J = 7.33 Hz, 1H), 6.97 (s, 1H), 7.04 (d, J = 8.34 Hz, 1H), 7.57 (d, J = 8.84 Hz, 1H). MS (APCI): 401 (M + H)⁺. Anal. calcd for $\text{C}_{21}\text{H}_{25}\text{ClN}_4\text{O}_2 \cdot 0.5\text{H}_2\text{O}$: C, 61.53; H, 6.39; N, 13.67. Found: C, 61.31; H, 6.38; N, 13.59.

Preparation of 21: *N*-[*trans*-3-(3-Chloro-4-cyanophenoxy)-2,2,4,4-tetramethylcyclobutyl]-5-methyl-1,3,4-oxadiazole-2-carboxamide. Compound **21** was prepared by the method of compound **30**, using 2-chloro-4-fluoro-benzonitrile (Aldrich, 344265) in step 1 and 5-methyl-[1,3,4]oxadiazole-2-carboxylic acid (Oakwood 047529) in step 2. $^1\text{H NMR}$ (400 MHz, CDCl_3): δ 1.22 (s, 6H), 1.30 (s, 6H), 2.66 (s, 3H), 4.08 (s, 1H), 4.13 (d, J = 8.84 Hz, 1H), 6.81 (dd, J = 8.72, 2.40 Hz, 1H), 6.97 (d, J = 2.27 Hz, 1H), 7.18 (d, J = 8.34 Hz, 1H), 7.58 (d, J = 8.84 Hz, 1H). MS (APCI): 389 (M + H)⁺. Anal. calcd for $\text{C}_{19}\text{H}_{21}\text{ClN}_4\text{O}_3 \cdot 1.0\text{H}_2\text{O}$: C, 56.09; H, 5.70; N, 13.77. Found: C, 56.46; H, 5.73; N, 13.41.

Preparation of 22: *N*-[*trans*-3-(3-Chloro-4-cyanophenoxy)-2,2,4,4-tetramethylcyclobutyl]imidazo[1,2-*a*]pyrimidine-3-carboxamide. Compound **22** was prepared by the method of compound **30**, using 2-chloro-4-fluoro-benzonitrile (Aldrich, 344265) in step 1. $^1\text{H NMR}$ (400 MHz, CDCl_3): δ 1.25 (s, 6H), 1.32 (s, 6H), 4.10 (s, 1H), 4.18 (d, J = 8.34 Hz, 1H), 6.09 (d, J = 8.08 Hz, 1H), 6.83 (dd, J = 8.59, 2.53 Hz, 1H), 6.99 (d, J = 2.53 Hz, 1H), 7.09 (dd, J = 6.95, 4.17 Hz, 1H), 7.59 (d, J = 8.59 Hz, 1H), 8.22 (s, 1H), 8.73 (dd, J = 4.29, 2.02 Hz, 1H), 9.76 (d, J = 5.05 Hz, 1H). MS (APCI): 424 (M + H)⁺. Anal. calcd for $\text{C}_{22}\text{H}_{22}\text{ClN}_5\text{O}_2 \cdot 1.15\text{H}_2\text{O}$: C, 59.43; H, 5.51; N, 15.75. Found: C, 59.19; H, 5.18; N, 15.60.

Preparation of 23: *N*-[*trans*-3-(3-Chloro-4-cyanophenoxy)-2,2,4,4-tetramethylcyclobutyl]-2-methylimidazo[1,2-*a*]pyrimidine-3-carboxamide. Compound **23** was prepared by the method of compound **30**, using 2-chloro-4-fluoro-benzonitrile (Aldrich, 344265) in step 1 and 2-methyl-imidazo[1,2-*a*]pyrimidine-3-carboxylic acid (Ryan Scientific, CA10041) in step 2. $^1\text{H NMR}$ (400 MHz, $\text{DMSO}-d_6$): δ 1.18 (s, 6H), 1.27 (s, 6H), 2.67 (s, 3H), 3.97 (d, J = 8.08 Hz, 1H), 4.34 (s, 1H), 7.03 (dd, J = 8.72, 2.40 Hz, 1H), 7.18 (dd, J = 6.95, 4.17 Hz, 1H), 7.24 (d, J = 2.27 Hz, 1H), 7.54 (d, J = 8.08 Hz, 1H), 7.91 (d, J = 8.59 Hz, 1H), 8.63

(dd, $J = 4.04, 2.02$ Hz, 1 H), 9.30 (dd, $J = 6.82, 2.02$ Hz, 1 H). MS (APCI): 438 (M + H)⁺. Anal. calcd for C₂₃H₂₄ClN₅O₂·0.5H₂O: C, 61.81; H, 5.64; N, 15.67. Found: C, 61.60; H, 5.53; N, 15.60.

Preparation of 24: *N*-[*trans*-3-(3-Chloro-4-cyanophenoxy)-2,2,4,4-tetramethylcyclobutyl]-1-(2-methoxyethyl)-1H-pyrazole-3-carboxamide. Compound **24** was prepared by the method of compound **30**, using 2-chloro-4-fluoro-benzonitrile (Aldrich, 344265) in step 1 and 2-methyl-imidazo[1,2-*a*]pyrimidine-3-carboxylic acid (Accel Pharm-tech, P7411) in step 2. ¹H NMR (400 MHz, DMSO-*d*₆): δ 7.81 (d, $J = 8.84$ Hz, 1 H), 7.73 (d, $J = 2.27$ Hz, 1 H), 7.22 (d, $J = 8.84$ Hz, 1 H), 7.15 (d, $J = 2.53$ Hz, 1 H), 6.93 (dd, $J = 8.84, 2.53$ Hz, 1 H), 6.56 (d, $J = 2.27$ Hz, 1 H), 4.32 (s, 1 H), 4.26 (t, $J = 5.31$ Hz, 2 H), 3.87 (d, $J = 8.84$ Hz, 1 H), 3.64 (t, $J = 5.31$ Hz, 2 H), 3.16 (s, 3 H), 1.11 (s, 6 H), 1.04 (s, 6 H). MS (APCI): 431.2 (M + H)⁺. Anal. calcd for C₂₂H₂₇ClN₄O₃: C, 61.32; H, 6.32; N, 13.00. Found: C, 61.18; H, 6.27; N, 12.85.

Preparation of 25: *N*-[*trans*-3-(3-Chloro-4-cyanophenoxy)-2,2,4,4-tetramethylcyclobutyl]-1-(2-hydroxyethyl)-1H-pyrazole-3-carboxamide. **Step 1. 1-(2-Hydroxyethyl)-1H-pyrazole-3-carboxylic Acid.** To a stirred solution of 3-bromo-1-propanol (Ryan Scientific, HA10111) (8.5 g, 0.068 mol) and a catalytic amount of TosOH in dry CH₂Cl₂ (30 mL) at 0 °C was added dihydropyran (DHP) (6.0 g, 0.071 mol) portion wise. After the addition, the mixture was stirred at the same temperature for more than 3 h. The resulting mixture was then diluted with CH₂Cl₂ (50 mL) and washed with water (20 mL × 2), aqueous NaHCO₃ (20 mL), and brine (30 mL), dried over anhydrous Na₂SO₄, and evaporated to give 2-(2-bromoethoxy)tetrahydro-2H-pyran (10 g, 70%) as yellow liquid, which was used for the next step directly.

The mixture of 1H-pyrazole-3-carboxylic acid methyl ester (Anichem C1398) (5.5 g, 0.0436 mol), 2-(2-bromoethoxy)tetrahydro-2H-pyran from step above (10.0 g, 0.048 mol), and K₂CO₃ (18.0 g, 0.13 mol) in CH₃CN (50 mL) was heated to reflux and stirred overnight. LC-MS test showed the reaction was complete. The precipitate was removed by filtration and washed with CH₃CN (50 mL × 2). The filtrate was concentrated and purified by flash chromatography with EtOAc/petroleum ether from 1/10 to 1/5 to give 2-(hydroxyethyl)-1H-pyrazole-3-carboxylic acid (3.0 g) and isomer methyl 1-(2-hydroxyethyl)-1H-pyrazole-5-carboxylate (5.0 g). A mixture of compound 2-(hydroxyethyl)-1H-pyrazole-3-carboxylic acid (3.0 g, 0.0118 mol) and concentrated HCl (1.96 mL) in MeOH (20 mL) was stirred at room temperature for more than an hour. The resulting mixture was concentrated to dryness to give the ester methyl 1-(2-hydroxyethyl)-1H-pyrazole-3-carboxylate, which was used for next step hydrolysis directly. The mixture of methyl 1-(2-hydroxyethyl)-1H-pyrazole-3-carboxylate (3.0 g, 0.0118 mol) and NaOH (1.18 g, 0.0295 mol) in the mixed solvent of water (10 mL) and MeOH (10 mL) was stirred at room temperature overnight. TLC analysis (1:1 petroleum ether:EtOAc) indicated that the reaction was complete. The mixture was concentrated. The residue was dissolved in water (150 mL) and extracted with EtOAc (20 mL × 2). The aqueous was acidified with concentrated HCl to pH 5 and concentrated. The crude product was then dissolved with EtOH (10 mL). The precipitate was removed by filtration. The filtrate was concentrated and recrystallized with 1/10 CH₂Cl₂/petroleum ether to afford 1-(2-hydroxyethyl)-1H-pyrazole-3-carboxylic acid (474 mg, 26%) as a yellow solid. ¹H NMR (400 MHz, D₂O): δ 7.76 (s, 1H), 6.89–6.88 (s, 1H), 4.36–4.33 (t, 2H), 3.99–3.96 (t, 2H). MS (APCI): 179.2 (M + H)⁺.

Step 2. N-[trans-3-(3-Chloro-4-cyanophenoxy)-2,2,4,4-tetramethylcyclobutyl]-1-(2-hydroxyethyl)-1H-pyrazole-3-carboxamide (25). Compound **25** was prepared by the method of compound **30**, using 2-chloro-4-fluoro-benzonitrile (Aldrich, 344265) in step 1 and 1-(2-hydroxyethyl)-1H-pyrazole-3-carboxylic acid (from step 1 above) in step 2. ¹H NMR (500 MHz, DMSO-*d*₆): δ 7.88 (d, $J = 8.78$ Hz, 1 H), 7.80 (br. s., 1 H), 7.25–7.30 (m, 1 H), 7.22 (br. s., 1 H), 7.03 (br. s., 1 H), 6.63 (br. s., 1 H), 4.90 (br. s., 1 H), 4.50–4.64 (m, 1 H), 4.40 (s, 1 H), 4.22 (t, $J = 5.61$ Hz, 2 H), 3.78 (br. s., 2 H), 1.19 (s, 6 H), 1.12 (s, 6 H). MS (APCI):

417.2 (M + H)⁺. Anal. calcd For C₂₁H₂₅ClN₄O₃·0.1H₂O: C, 65.73; H, 6.28; N, 20.00. Found: C, 65.41; H, 6.29; N, 19.94.

Preparation of 26: *N*-[*trans*-3-(3-Chloro-4-cyanophenoxy)-2,2,4,4-tetramethylcyclobutyl]-1-(2-hydroxyethyl)-1H-pyrazole-4-carboxamide. Compound **26** was prepared by the method of compound **30**, using 2-chloro-4-fluoro-benzonitrile in step 1 and 1-(2-hydroxy-ethyl)-1H-pyrazole-4-carboxylic acid (Ryan Scientific, BBV-074900) in step 2. ¹H NMR (400 MHz, DMSO-*d*₆): δ ppm 1.10 (s, 6 H), 1.20 (s, 6 H), 3.74 (q, $J = 5.22$ Hz, 2 H), 4.06 (d, $J = 9.35$ Hz, 1 H), 4.16 (t, $J = 5.43$ Hz, 2 H), 4.29 (s, 1 H), 4.94 (t, $J = 5.05$ Hz, 1 H), 7.01 (dd, $J = 8.84, 2.27$ Hz, 1 H), 7.21 (d, $J = 2.27$ Hz, 1 H), 7.33 (d, $J = 9.60$ Hz, 1 H), 7.90 (d, $J = 8.84$ Hz, 1 H), 7.92 (s, 1 H), 8.28 (s, 1 H). HRMS: [M + H]⁺ calcd, 417.168795; found, 417.169311; error, 1.24. Anal. calcd for C₂₁H₂₅ClN₄O₃: C, 60.50; H, 6.04; N, 13.44; Cl, 8.50. Found: C, 60.43; H, 6.22; N, 13.51; Cl, 8.39.

Preparation of 27: *N*-[*trans*-3-(3-Chloro-4-cyanophenoxy)-2,2,4,4-tetramethylcyclobutyl]-1-(2-cyanoethyl)-1H-pyrazole-3-carboxamide. **Step 1. Synthesis of 1-(2-Cyano-ethyl)-1H-pyrazole-3-carboxylic Acid.** A solution of pyrazole-3-carboxylic acid methyl ester (588.7 mg, 4.668 mmol), acrylonitrile (0.62 mL, 9.41 mmol), and DBU (0.35 mL, 2.3 mmol) in acetonitrile (2.3 mL) was stirred in a sealed tube at room temperature for 26 h. After evaporation and purification by silica gel chromatography (eluting with 50–100% ethyl acetate in heptane), 1-(2-cyano-ethyl)-1H-pyrazole-3-carboxylic acid methyl ester (803.9 mg, 96%) was obtained as a white solid. ¹H NMR (400 MHz, DMSO-*d*₆): δ 3.12 (t, $J = 6.44$ Hz, 2 H), 3.80 (s, 3 H), 4.49 (t, $J = 6.44$ Hz, 2 H), 6.79 (d, $J = 2.27$ Hz, 1 H), 7.96 (d, $J = 2.27$ Hz, 1 H). A portion of this ester (692.6 mg, 3.865 mmol) was saponified with lithium hydroxide monohydrate (220.3 mg, 5.25 mmol) in methanol (15.4 mL) at room temperature for 26 h. The reaction was diluted with 10 mL of deionized water, the methanol was evaporated, and the residue was partitioned between ethyl acetate (20 mL) and saturated aqueous NaHCO₃ (15 mL). The organic layer was discarded, and the aqueous layer treated dropwise with 6 N HCl until pH ~1. The now-acidic aqueous layer was extracted with ethyl acetate (3 × 20 mL). These extracts were combined, dried over magnesium sulfate, filtered, and concentrated to give 1-(2-cyano-ethyl)-1H-pyrazole-3-carboxylic acid (432.1 mg, 67%) as a white solid. ¹H NMR (400 MHz, DMSO-*d*₆): δ 3.11 (t, $J = 6.44$ Hz, 2 H), 4.47 (t, $J = 6.44$ Hz, 2 H), 6.72 (d, $J = 2.27$ Hz, 1 H), 7.91 (d, $J = 2.27$ Hz, 1 H), 12.71 (s, 1 H).

Step 2. N-[trans-3-(3-Chloro-4-cyanophenoxy)-2,2,4,4-tetramethylcyclobutyl]-1-(2-cyanoethyl)-1H-pyrazole-3-carboxamide (27). Compound **27** was prepared by the method of compound **30**, using 2-chloro-4-fluoro-benzonitrile in step 1 and 1-(2-cyano-ethyl)-1H-pyrazole-3-carboxylic acid (see step 1 above) in step 2. ¹H NMR (400 MHz, DMSO-*d*₆): δ 1.12 (s, 6 H), 1.20 (s, 6 H), 3.13 (t, $J = 6.44$ Hz, 2 H), 3.96 (d, $J = 8.84$ Hz, 1 H), 4.39 (s, 1 H), 4.48 (t, $J = 6.44$ Hz, 2 H), 6.70 (d, $J = 2.27$ Hz, 1 H), 7.02 (dd, $J = 8.72, 2.40$ Hz, 1 H), 7.23 (d, $J = 2.53$ Hz, 1 H), 7.33 (d, $J = 8.84$ Hz, 1 H), 7.89 (d, $J = 8.59$ Hz, 1 H), 7.93 (d, $J = 2.27$ Hz, 1 H). HRMS: [M + H]⁺ calcd, 426.169129; found, 426.169823; error, 1.63 ppm.

Preparation of 28: *N,N*-[*trans*-3-(3-Chloro-4-cyanophenoxy)-2,2,4,4-tetramethylcyclobutyl]-1-[2-(methylamino)-2-oxoethyl]-1H-pyrazole-3-carboxamide. Compound **28** was prepared by the method of compound **30**, using 2-chloro-4-fluoro-benzonitrile (Aldrich, 344265) in step 1 and 1-(2-(methylamino)-2-oxoethyl)-1H-pyrazole-3-carboxylic acid (Chemcollect, ChemCol-MC006604). ¹H NMR (500 MHz, DMSO-*d*₆): δ 1.10–1.14 (m, 6 H), 1.19 (br. s., 6 H), 2.63 (d, $J = 4.39$ Hz, 3 H), 3.95 (d, $J = 8.78$ Hz, 1 H), 4.38 (br. s., 1 H), 4.87 (br. s., 2 H), 6.62–6.74 (m, 1 H), 7.01 (d, $J = 8.30$ Hz, 1 H), 7.21 (br. s., 1 H), 7.28 (d, $J = 8.78$ Hz, 1 H), 7.71–7.81 (m, 1 H), 7.84–7.90 (m, 1 H), 8.03 (br. s., 1 H). MS (APCI): 444.2 (M + H)⁺. Anal. calcd For C₂₂H₂₆ClN₅O₃·0.25H₂O: C, 58.93; H, 5.96; N, 15.62. Found: C, 58.81; H, 5.96; N, 15.49.

Preparation of 29: *N*-[*trans*-3-(3-Chloro-4-cyanophenoxy)-2,2,4,4-tetramethylcyclobutyl]-1-[2-(dimethylamino)-2-oxoethyl]-1H-pyrazole-3-carboxamide. Compound **29** was prepared by the method of

compound **30**, using 2-chloro-4-fluoro-benzonitrile (Aldrich, 344265) in step 1 and 1-(2-(dimethylamino)-2-oxoethyl)-1H-pyrazole-3-carboxylic acid (ChemCollect, ChemCol-MC006605). ¹H NMR (500 MHz, DMSO-*d*₆): δ 1.11 (br. s., 6 H), 1.18 (br. s., 6 H), 2.86 (br. s., 3 H), 3.03 (br. s., 3 H), 3.96 (d, *J* = 8.30 Hz, 1 H), 4.38 (br. s., 1 H), 5.21 (br. s., 2 H), 6.66 (br. s., 1 H), 7.01 (d, *J* = 8.30 Hz, 1 H), 7.13–7.34 (m, 2 H), 7.73 (br. s., 1 H), 7.82–8.01 (m, 1 H). MS (APCI): 458.2 (M + H)⁺. Anal. calcd for C₂₃H₂₈ClN₅O₃·0.5H₂O: C, 59.16; H, 6.26; N, 15.00. Found: C, 59.12; H, 6.21; N, 14.72.

Computational Model Used for Docking Compound 5 in AR Helix 12-Closed Conformation. The AR protein model for Figure 6 was based on the AR-bicalutamide crystal structure (PDB code: 1Z95) where helix 12 was removed (starting at Lys-883) to accommodate induced-fit docking of RD-162 where residues within 6 Å of the ligand are allowed to relax (unpublished routine in AGDOCK). Compound **5** was docked into this relaxed structure using the AGDOCK^{18,19} docking program.

Computational Model Used for Docking Compounds 5 and 30 (Figure 11) in AR Helix 12-Open Conformation. The AR homology model was built based on Raloxifene bound ER crystal structure (PDB code: 1ERR) using the PRIME homology modeling program. The side chain coordinate and the loop conformation were explored and optimized in the same program. Docking simulation was performed with Glide docking program,²⁰ and compounds were docked into a binding pocket of bicalutamide in AR crystal structure (PDB code: 1Z95) and the homology model.

■ ASSOCIATED CONTENT

Supporting Information. Schemes of the synthesis of cyclobutyl intermediate **7** and the representative procedure for the synthesis of cyclobutyl analogues, general experimental section, and characterization of final analogues. This material is available free of charge via the Internet at <http://pubs.acs.org>.

■ AUTHOR INFORMATION

Corresponding Authors

*Tel: 858-622-5927. E-mail: Alex.Guo@pfizer.com (C.G.). Tel: 858-622-7913. E-mail: Angelica.Linton@pfizer.com (A.L.).

■ ACKNOWLEDGMENT

We thank Chris Bi for coordinating CRO synthesis of the general intermediate **7**.

■ ABBREVIATIONS USED

ADME, absorption, distribution, metabolism, and elimination; AR, androgen receptor; CRPC, castration-resistant prostate cancer; DHT, dihydrotestosterone; DMSO, dimethyl sulfoxide; ER, estrogen receptor; FBS, fetal bovine serum; HLM, human liver microsomes; HRPC, hormone refractory prostate cancer; LBD, ligand binding domain; LE, ligand efficiency based on number of heavy atoms; LipE, ligand efficiency based on lipophilicity; NHRM, nuclear hormone receptor; PD, pharmacodynamic; PK, pharmacokinetic; PSA, prostate specific antigen; QD, once a day dosing; SAR, structure–activity relationship

■ REFERENCES

(1) Chen, Y.; Sawyers, C. L.; Scher, H. I. Targeting the androgen receptor pathway in prostate cancer. *Curr. Opin. Pharmacol.* **2008**, *8*, 440–448.

(2) Schellhammer, P. An update on bicalutamide in the treatment of prostate cancer. *Expert Opin. Invest. Drugs* **1999**, *8*, 849–860.

(3) (a) Kelly, W. K.; Slovin, S.; Scher, H. I. Steroid hormone withdrawal syndromes. Pathophysiology and clinical significance. *Urol. Clin. North Am.* **1997**, *24*, 421–431. (b) Chen, C. D.; Welsbie, D. S.; Tran, C.; Baek, S. H.; Chen, R.; Vessella, R.; Rosenfeld, M. G.; Sawyers, C. L. Molecular determinants of resistance to antiandrogen therapy. *Nat. Med.* **2004**, *10*, 33–39.

(4) (a) Jung, M. E.; Ouk, S.; Yoo, D.; Sawyers, C. L.; Chen, C.; Tran, C.; Wongvipat, J. Structure-activity relationship for thiohydantoin androgen receptor antagonists for castration-resistant prostate cancer (CRPC). *J. Med. Chem.* **2010**, *53*, 2779–96. (b) Tran, C.; Ouk, S.; Clegg, N. J.; Chen, Y.; Watson, P. A.; Arora, V.; Wongvipat, J.; Smith-Jones, P. M.; Yoo, D.; Kwon, A.; Wasielewska, T.; Welsbie, D.; Chen, C. D.; Higano, C. S.; Beer, T. M.; Hung, D. T.; Scher, H. I.; Jung, M. E.; Sawyers, C. L. Development of a second-generation antiandrogen for treatment of advanced prostate cancer. *Science* **2009**, *324*, 787–790.

(5) (a) Attar, R. M.; Jure-Kunkel, M.; Balog, A.; Cvijic, M. E.; Dell-John, J.; Rizzo, C. A.; Schweizer, L.; Spiers, T. E.; Platero, J. S.; Obermeier, M.; Shan, W.; Salvati, M. E.; Foster, W. R.; Dinchuk, J.; Chen, S. J.; Vite, G.; Kramer, R.; Gottardis, M. M. Discovery of BMS-641988, a novel and potent inhibitor of androgen receptor signaling for the treatment of prostate cancer. *Cancer Res.* **2009**, *69*, 6522–6530. (b) Salvati, M. E.; Balog, A.; Shan, W.; Rampulla, R.; Giese, S.; Mitt, T.; Furch, J. A.; Vite, G. D.; Attar, R. M.; Jure-Kunkel, M.; Geng, J.; Rizzo, C. A.; Gottardis, M. M.; Krystek, S. R.; Gougoutas, J.; Galella, M. E.; Obermeier, M.; Fura, A.; Chandrasena, G. Identification and optimization of a novel series of [2.2.1]-oxabicyclo imide-based androgen receptor antagonists. *Bioorg. Med. Chem. Lett.* **2008**, *18*, 1910–1915. (c) Salvati, M. E.; Balog, A.; Shan, W.; Wei, D. D.; Pickering, D.; Attar, R. M.; Geng, J.; Rizzo, C. A.; Gottardis, M. M.; Weinmann, R.; Krystek, S. R.; Sack, J.; An, Y.; Kish, K. Structure based approach to the design of bicyclic-1H-isoindeole-1,3(2H)-dione based androgen receptor antagonists. *Bioorg. Med. Chem. Lett.* **2005**, *15*, 271–276. (d) Salvati, M. E.; Balog, A.; Wei, D. D.; Pickering, D.; Attar, R. M.; Geng, J.; Rizzo, C. A.; Hunt, J. T.; Gottardis, M. M.; Weinmann, R.; Martinez, R. Identification of a novel class of androgen receptor antagonists based on the bicyclic-1H-isoindeole-1,3(2H)-dione nucleus. *Bioorg. Med. Chem. Lett.* **2005**, *15*, 389–393.

(6) Scher, H. I.; Beer, T. M.; Higano, C. S.; Anand, A.; Taplin, M. E.; Efstathiou, E.; Rathkopf, D.; Shelkey, J.; Yu, E. Y.; Alumkal, J.; Hung, D.; Hirmand, M.; Seely, L.; Morris, M. J.; Danila, D. C.; Humm, J.; Larson, S.; Fleisher, M.; Sawyers, C. L. Prostate Cancer Foundation/Department of Defense Prostate Cancer Clinical Trials Consortium. *Lancet* **2010**, *375*, 1437–1446.

(7) CRPC cell-based HTS assay: In this assay, prostate cancer refractory cells (LNAR), stably expressing an AR response element DNA sequence (ARE)-luciferase reporter gene construct (ARE2-PB-Luc), and overexpressing wild-type human AR were treated with the testing compounds in the absence (agonistic mode) or the presence (antagonistic mode) of a potent agonist (R1881). Upon activation and binding of the AR to the ARE, the luciferase gene transcribed and translated into active luciferase enzyme and luminescence was read as a signal by the plate reader. Testing compounds were dissolved in 100% dimethyl sulfoxide (DMSO) as 10 mM stock solution. Serial dilutions were prepared from 0.17 nM to 10 μM, and the final DMSO concentration never exceeded 0.1%. For agonism, values obtained from the compounds under study were compared to those of untreated cells, which were assigned an arbitrary number of 1.0 to indicate no agonism. For antagonism, cells were treated with 0.1 nM R1881 alone (corresponding to max receptor activation = 100%) or in combination with the various compounds.

(8) The cutoff for significant residual AR agonism was set to >1.032-fold induction in CRPC cell-based assay (agonism mode, see ref 7) based on statistic analysis of multiple test results (*n* = 176) of RD162 in the same assay. RD-162, a full AR antagonist reported in the literature (refs 4a and 4b), was used as a reference standard. In the agonism assay, the averaged agonism fold induction of RD162 (*n* = 176) is 0.876 with a standard deviation of 0.0779. An AR ligand with an agonism fold induction >1.032 (0.876 + 2 × 0.0779) is likely (>95% confidence) to have more residual agonism than RD162.

(9) Ryckmans, T.; Edwards, M. P.; Horne, V. A.; Correia, A. M.; Owen, D. R.; Thompson, L. R.; Tran, L.; Tutt, M. F.; Young, T. Rapid assessment of a novel series of selective CB(2) agonists using parallel synthesis protocols: A Lipophilic Efficiency (LipE) analysis. *Bioorg. Med. Chem. Lett.* **2009**, *19*, 4406–4409.

(10) HLM data shown in this paper are the intrinsic metabolic clearance (Clint) in microsomes, in $\mu\text{L}/\text{min}/\text{mg}$ of microsomal protein. Data interpretation as was follows: Clint $< 15 \mu\text{L}/\text{min}/\text{mg}$ (low clearance); Clint $15\text{--}40 \mu\text{L}/\text{min}/\text{mg}$ (moderate clearance); Clint >40 (high clearance).

(11) LNCaP xenograft model of CRPC: Male athymic nude mice (Harlan Sprague–Dawley, Inc.) were injected subcutaneously with 1 million LNCaP cells in both flanks. Body weight, tumor volume, and serum prostate specific antigen (PSA) values were followed weekly. Mice were castrated once tumors reached between 300 and 500 mm^3 or the PSA level was $>50 \text{ ng/mL}$. Once tumors progressed to androgen independence, defined by PSA levels returning to precastration values, mice were randomly assigned to vehicle or various drugs and treatments started. Treatment was per oral (po) and administered once daily in a formulation containing 0.9% benzyl alcohol, 1% Tween-80, and 98.1% methylcellulose (0.5%). PSA and tumor volume were measured once and twice weekly, respectively. The tumor volume was calculated by the formula: length \times width \times depth \times 0.5236. To calculate tumor growth inhibition, the following formula was used: inhibition (%) = (TuG control – TuG test)/TuG control \times 100%, where tumor growth (TuG) equals the final tumor size minus the pretreatment tumor size for individual treatment groups. Serum PSA levels were determined by using the PSA ELISA Kit (American Qualex Antibodies, catalog no. KD4310) following the manufacturer's instructions.

(12) Stephan, C.; Cammann, H.; Meyer, H. A.; Lein, M.; Jung, K. PSA and new biomarkers within multivariate models to improve early detection of prostate cancer. *Cancer Lett.* **2007**, *249*, 18–29.

(13) Pereira De Jesus-Tran, K.; Cote, P.; Cantin, L.; Blanchet, J.; Labrie, F.; Breton, R. Comparison of crystal structures of human androgen receptor-ligand domain complexed with various agonists reveals molecular determinants responsible for binding affinity. *Protein Sci.* **2006**, *15*, 987–999.

(14) (a) De Bellis, A.; Quigley, C. S.; Cariello, N. F.; El-Awady, M. K.; Sar, M.; Lane, M. V.; Wilson, E. M.; French, F. S. Single base mutations in the androgen receptor gene causing complete androgen insensitivity: Rapid detections by a modified denaturing gradient gel electrophoresis technique. *Mol. Endocrinol.* **1992**, *6*, 1909–1920. (b) Pinsky, L.; Trifiro, M.; Kaufman, M.; Beitel, L. K.; Mhatre, A.; Kazemi-Esfarjani, P.; Sabbaghian, N.; Lumbroso, R.; Alvarado, C.; Vasiliou, M.; et al. Androgen resistance due to mutation of the androgen receptor. *Clin. Invest. Med.* **1992**, *15*, 456–472. (c) Hur, E.; Pfaff, S. J.; Payne, E. S.; Gron, H.; Buehrer, B. M.; Fletterick, R. J. Recognition and accommodation at the androgen receptor coactivator binding interface. *PLoS Biol.* **2004**, *2*, E274.

(15) (a) Shiao, A. K.; Barstad, D.; Loria, P. M.; Cheng, L.; Kushner, P. J.; Agard, D. A.; Greene, G. L. The Structural Basis of Estrogen Receptor/Coactivator Recognition and the Antagonism of This Interaction by Tamoxifen. *Cell* **1998**, *95*, 927–937. (b) Webb, P.; Nguyen, N.; Chiellini, G.; Yoshihara, H. A. I.; Cunha Lima, S. T.; Apriletti, J. W.; Ribeiro, R. C. J.; Marimuthu, A.; West, B. L.; Goede, P.; Mellstrom, K.; Nilsson, S.; Kushner, P. J.; Fletterick, R. J.; Scanlan, T. S.; Baxter, J. D. Design of thyroid hormone receptor antagonists from first principles. *J. Steroid Biochem. Mol. Biol.* **2003**, *83*, 59–73. (c) Pike, A. C. W.; Brzozowski, A. M.; Hubbard, R. E.; Bonn, T.; Thorsell, A. G.; Engstro, O.; Ljunggren, J.; Gustafsson, J.; Carlquist, M. Structure of the ligand binding domain of oestrogen receptor beta in the presence of a partial agonist and a full antagonist. *EMBO J.* **1999**, *18*, 4608–4618. (d) Schoch, G. A.; D'Arcy, B.; Stihle, M.; Burger, D.; Bar, D.; Benz, J.; Thoma, R.; Ruf, A. Molecular Switch in the Glucocorticoid Receptor: Active and Passive Antagonist Conformations. *J. Mol. Biol.* **2010**, *568*–577.

(16) The preparation of 7 is found in the Supporting Information.

(17) The unbound C_{ave} is the free averaged drug concentration in plasma, which was calculated with following formula: $(1 - \text{plasma protein binding}) \times (\text{AUC}_{0-24 \text{ h}}/24 \text{ h})$.

(18) Gehlhaar, D. K.; Verkhivker, G. M.; Rejto, P. A.; Sherman, C. J.; Fogel, D. B.; Fogel, L. J.; Freer, S. T. Molecular Recognition of the Inhibitor AG-1343 by HIV-1 Protease: Conformationally Flexible Docking by Evolutionary Programming. *Chemistry and Biology* **1995**, *2* (5), 317–324.

(19) Gehlhaar, D. K.; Bouzida, D.; Rejto, P. A. Reduced Dimensionality in Ligand-Protein Structure Prediction: Covalent Inhibitors of Serine Proteases and Design of Site-Directed Combinatorial Libraries; ACS Symposium Series 719: Rational Drug Design. Parrill, A. L. and M. R. Reddy, Eds. ACS Press, 1999, 292–311.

(20) *Glide*, version 5.5, Schrodinger, Inc., New York, NY, 2009.